Highly Efficient Wideband mmWave Rectennas for Wireless Power Transfer System With Low-Cost Multinode Tracking Capability

Chaoyun Song, *Senior Member, IEEE*, Lei Wang, *Senior Member, IEEE*, Ping Lu, *Member, IEEE*, Cheng Zhang, *Member, IEEE*, Zhensheng Chen, Xuezhi Zheng, *Member, IEEE*, Yejun He, *Senior Member, IEEE*, George Goussetis, *Senior Member, IEEE*, Guy A. E. Vandenbosch, *Fellow, IEEE*, and Yi Huang, *Fellow, IEEE*

***Abstract*—An innovative wireless power transfer (WPT) system utilizing millimeter-wave (mmWave) power for multinode charging and tracking is presented in this article. The core concept of the system revolves around the utilization of frequency-dispersive leaky-wave antenna (LWA) transmitters, enabling passive beam scanning in the far field without the need for active phased arrays. However, such a system requires a breakthrough in receiving rectenna design at mmWave frequencies, encompassing a wide frequency bandwidth, wide beamwidth, and high RF-to-dc conversion efficiency beyond 20 GHz. In this work, we introduce a pioneering mmWave rectenna design achieved through the codesign integration of a magnetoelectric (ME) dipole and high-frequency diodes, eliminating the need for complex impedance matching networks at mmWave frequencies. The proposed rectenna operates in the frequency range of 24–34.5 GHz, achieving over 50% RF-to-dc conversion efficiency for input powers exceeding 15 dBm. In addition, the rectenna demonstrates improved gain and beamwidth compared to conventional designs, enabling wide-angle reception of frequency-scanning passively beamformed mmWave signals. A practical demonstration of the proposed system showcases simultaneous wireless charging of three nodes, highlighting its notable advantages in terms of mobility, cost-effectiveness, and simplicity over conventional WPT technologies.**

***Index Terms*—Leaky-wave antenna (LWA), mmWave, node tracking, rectennas, wireless power transfer (WPT).**

Manuscript received 19 July 2023; revised 29 August 2023; accepted 1 September 2023. Date of publication 13 September 2023; date of current version 30 October 2023. This work was supported in part by the King's College London (KCL) Starting Grant; in part by the National Natural Science Foundation of China (NSFC) under Grant 62071306; and in part by the Shenzhen Science and Technology Program under Grant JCYJ20200109113601723, Grant JSGG20210802154203011, and Grant JSGG20210420091805014. *(Corresponding author: Chaoyun Song.)*

Chaoyun Song is with the Department of Engineering, King's College London, Strand Campus, WC2R 2LS London, U.K., and also with the State Key Laboratory of Radio Frequency Heterogeneous Integration, College of Electronics and Information Engineering, Shenzhen University, Shenzhen 518060, China (e-mail: chaoyun.song@kcl.ac.uk).

Lei Wang and George Goussetis are with the School of Engineering and Physical Sciences, Heriot-Watt University, EH14 4AS Edinburgh, Scotland, U.K.

Ping Lu is with the School of Electronics and Information Engineering, Sichuan University, Chengdu 610064, China.

Cheng Zhang is with the Shanghai Institute of Optics and Fine Mechanics, Chinese Academy of Sciences, Shanghai 201800, China.

Zhensheng Chen, Xuezhi Zheng, and Guy A. E. Vandenbosch are with the Department of Electrical Engineering (ESAT), KU Leuven, 3001 Leuven, Belgium.

Yejun He is with the State Key Laboratory of Radio Frequency Heterogeneous Integration, Sino-British Antennas and Propagation Joint Laboratory, Shenzhen Key Laboratory of Antennas and Propagation, Guangdong Engineering Research Center of Base Station Antennas, College of Electronics and Information Engineering, Shenzhen University, Shenzhen 518060, China.

Yi Huang is with the Department of Electrical Engineering and Electronics, University of Liverpool, L69 3BX Liverpool, U.K.

Color versions of one or more figures in this article are available at https://doi.org/10.1109/TAP.2023.3313182.

Digital Object Identifier 10.1109/TAP.2023.3313182

I. Introduction

Wireless power transfer (WPT) has a transformative potential to simplify our everyday life as it increases mobility, convenience, and safety for plenty of applications in consumer electronics, electric vehicles, defense, and space technologies [1]. The development of WPT technology has been historically important, which started with Tesla's heritage experiment in the 1890s, and has experienced an over 100 years' roadmap with many significant achievements and milestones [2], [3], [4], [5], [6]. In recent decades, the emergence of the Qi standard in 2010 enabled vast ranges of smartphones and wearable devices with wireless charging capabilities [7], [8]. However, user benefits largely rely on the elimination of cords and wires but fall short of providing the flexibility of truly remote (charging distance >20 cm) and on-the-move charging of handheld devices. The hunt for remote and on-the-move charging is on [9].

Far-field WPT via radio waves is a promising way for remote charging (e.g., up to kilometers for Space Solar Power Satellites [10]). However, the radiative wireless power could be largely scattered in open areas, while the path loss of radio waves propagating in free space is significant; consequently, the end-to-end efficiency of the far-field WPT system is relatively low. This has been the main challenge for traditional radiative power transfer. To improve the WPT link efficiency, high directivity antenna arrays with beamforming capabilities are preferred to transmit power effectively. State-of-the-art research has shown the feasibility of using the phased array [11], [12], [13], [14], [15] and digital metasurfaces [16], [17], [18] for wireless power beamforming and near-field beam focusing such that the power beam could be focused sharply, while the beam direction is switchable toward several receiver locations. However, the phased array concept essentially needs active phase shifters and array feeding networks, which introduces significant power loss (more than 6 dB) and increases the costs tremendously. Similarly, digital metasurface and beamformers for radiative near-field focusing need the massive integration of p-i-n diodes and costly semiconductor varactors, thereby reducing the WPT efficiency and charging distances. The beam scanning range, the number of beam directions, and the beam scanning resolution of both technologies are directly determined by how many active phase shifters and switches are integrated into the design. These significant drawbacks in terms of high complexity, high power loss, and high cost have become the bottleneck when applying such far-field WPT in real-world applications.

Node tracking is crucial when wirelessly remote charging a moving target. This will need the feedback information sent from the receiver to effectively control the wireless power beamforming at the transmitter. Existing studies have demonstrated the use of retrodirective antenna arrays (RDA) for node tracking [19], [20]. An RDA automatically retransmits a signal toward a source without prior knowledge of the incoming signal. Due to the need for phase conjugation to realize retrodirectivity, RDAs typically consist of signal mixers, subarrays, multiple power amplifiers (PAs), and bandpass filters [19]. This might bring in extra costs, power loss, and complexity for the WPT systems. Time reversal (TR) is another emerging technology for selectively delivering wireless power to the targeted nodes. Different from the phased array that relies on phase shifting, TR transmitting arrays operate in a switching manner where only one element transmits at a time [21], [22]. The node selectivity is accomplished by measuring the feedback beacon signal sent from the receiver and correspondingly selecting the optimal transmitting antenna element. However, both RDA and TR technologies need large active antenna arrays consisting of multiple antenna elements, PAs, and complex feedings. They still need to be actively controlled and/or switched, which inherently has a higher cost and higher power loss compared to the conventional passive transmitting antenna.

Therefore, having considered all state-of-the-art technologies, the major challenges for far-field radiative WPT are summarized as follows.

1) How to increase the WPT efficiency and power delivery at larger distances?

2) How to enable node tracking and beamforming for the WPT system with low-cost and low-power loss methods?

3) How to effectively establish a multitarget WPT system with excellent simplicity, cost-effectiveness, and reliability?

To address these grand challenges, in this article, we will present a brand-new WPT system using millimeter-wave (mmWave) signals. The benefits of mmWave WPT in terms of relaxed effective isotropic radiated power (EIRP) level, higher efficiency, and higher deliverable power will be introduced in Section II. Importantly, we will propose a novel passive beamforming method by exploiting the inherent frequency dispersion nature of leaky wave antenna (LWA) transmitters [34], [35], thereby eliminating the need for active phased array transmitters that exhibit extremely high-cost and high-power loss at mmWave frequencies.

Antenna size: Transmitting: 20 cm Receiving: 4 cm WPT distance: 5 m	Conventional microwave WPT (at 3 GHz)	The Proposed mmWave WPT (at 30 GHz)	Improvement rate (dB or %)
TX antenna gain	13 dBi	30 dBi	17 dB
RX antenna gain	2 dBi	10 dBi	8 dB
EIRP Limit	36 dBm	75 dBm	39 dB
Max. TX power	23 dBm	45 dBm	22 dB
Max. RX power	-18 dBm	9 dBm	27 dB
WPT efficiency	**$7.5\text{X}10^{-3}$ %**	**$2.5\text{X}10^{-2}$ %**	**333%**
Path Loss	**41 dB**	**36 dB**	**5 dB**
Beam scanning loss	>6 dB	0 dB	6 dB

Fig. 1. Comparison between conventional WPT system at 3 GHz and the proposed WPT system at 30 GHz. Note that the WPT efficiency here is the RF-RF power transfer efficiency at 5 m without considering the rectification.

At the receiver end, we will present a newly designed wideband and wide-beam mmWave rectenna to efficiently capture the spectrum-sweeping signals transmitted from the LWA (Section III). It is worth noting that wideband mmWave rectennas with high conversion efficiency have not been widely reported [23], [24]. Only a limited number of works have demonstrated good power conversion efficiency exceeding 30% and wide bandwidth [25], [26], [27], [28], [29], [30], [31]. In this article, we conduct an in-depth theoretical and experimental investigation of the codesigning strategy involving a magnetoelectric (ME) dipole and high-frequency diodes over a wide mmWave spectrum from 20 to 40 GHz, thereby for the first time reporting a highly efficient (>50%), wide beamwidth (>90°) and wideband (34.5% bandwidth) mmWave rectenna. The experimental verification of the proposed mmWave rectenna is presented in Section IV.

Moreover, a preliminary demonstration for the proposed multitarget wireless charging and node tracking system is showcased in Section V. Three nodes can be wirelessly powered simultaneously with a closed control loop using the dc power monitor for the rectenna, feedback beacon signals, and multifrequency modulation and sweeping for the transmitting mmWave signals. Finally, conclusions are drawn in Section VI.

II. Wideband mmWave WPT

A. Why mmWave?

Compared to sub-6-GHz bands, the EIRP limit of mmWave band is increased from 36 to 75 dBm (according to FCC and 3GPP) [26]. This means that the mmWave power transmitter could radiate significantly enhanced power (about 39 dB higher) in domestic environments within safety human exposure constraints. In addition, mmWave antennas offer the advantage of achieving higher directivity (>25 dBi) with a given aperture size. Furthermore, mmWave RF devices naturally have smaller overall dimensions compared to microwave devices. For instance, the wavelength at 3 GHz is ten times larger than that at 30 GHz, resulting in a reduced physical size of mmWave devices. Hence, a high directivity mmWave WPT system may have better end-to-end efficiency as well as much higher deliverable wireless power at identical distances compared with microwave systems. In Fig. 1, we have

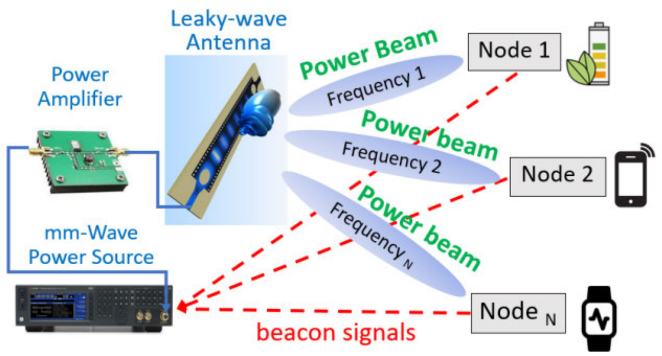

Fig. 2. Proposed multitarget WPT system using mmWave power. The system consists of an LWA, PA, signal source, and mmWave wideband wide-beam rectennas. The feedback beacon signal is used for multinode tracking.

compared the performance of a typical WPT system at 3 GHz with that of our proposed system at 30 GHz. We assume that both systems have an identical transmitting aperture side of 20 cm and a receiving aperture size of 4 cm. The conventional 3-GHz system was estimated using a microstrip patch antenna array [32]. At an identical power transfer distance of 5 m, the proposed mmWave system will have 27 dB more received power, 5 dB less path loss, and 333% efficiency improvement. The free-space path loss can be greatly mitigated by high directivity and high aperture efficiency of mmWave antennas, while the transmitting power is enhanced by the relaxed EIRP regulations. However, the major challenges for mmWave WPT are the cost, power loss, and efficiency of mmWave PAs, phase shifters, and active switches. It is overly expensive to build the power beamforming and node tracking capabilities for the remote charging system at mmWave frequencies using conventional technologies, and for this reason, it has not yet been substantially explored [33]. The active beam scanning loss (e.g., phased array) at 3 GHz will be more than 6 dB and it will be even higher at 30 GHz.

B. Novelty and Advantages

The proposed system architecture is shown in Fig. 2. In this study, our focus is on utilizing a passive beam-scannable and beam-formable antenna called the LWA. The LWA is a type of traveling-wave antenna that relies on a guiding structure to support wave propagation along its length, with the wave continuously or periodically radiating/leaking along the structure. It exhibits natural frequency-dependent beam scanning and exceptional radiation efficiency (>90%) at mmWave frequency bands [34], [35]. Although the frequency-dispersive nature of the LWA presents challenges in typical wireless communications, we can leverage this characteristic for WPT. Specifically, we can develop a wideband wide-beam rectenna (power receiver) capable of capturing frequency-dependent power beams emitted by the LWA transmitter. By employing this approach, beamforming of the LWA power transmitter can be accomplished simply by adjusting the frequency of the mmWave signals. This approach offers significant advantages over conventional active beam scanning, near-field focusing, and other WPT beamforming methods, including reduced power loss, cost, and complexity. In our proposed system, multitarget tracking can be achieved through multitone frequency modulation and sweeping, with real-time control based on feedback signals received from the rectennas.

The core concept involves identifying the synchronized instance for delivering the peak dc power to the rectenna and shaping the power beam according to the frequency spectrum. Further details regarding this approach will be provided in Section V. However, it is evident that the primary challenge lies in designing highly efficient wideband and wide-beam rectennas for mmWave bands. This challenge forms the main focus of our research.

III. Wideband Wide-Beam mmWave Rectenna Design

In the proposed WPT system, the receiving rectennas will undoubtedly become the most challenging part to be dealt with. One reason is due to the requirement for high RF-to-dc conversion efficiency across large frequency bandwidth to cope with the wide-angle scanning beams radiated from the frequency-scanning LWAs. Another critical concern is around the tradeoffs between half power beamwidth and directivity of the receiver, in which the broadband rectenna is ideally of high gain and wide beam. More importantly, the proposed antenna will need to operate at a wide mmWave spectrum for frequencies >20 GHz, thereby posing significant challenges in terms of the rectifier design by using high-frequency diodes.

To date, there is a very limited number of mmWave rectennas published in the open literature, while very few works can operate effectively over a large bandwidth. A valuable conclusion summarized from the existing work is that the rectifiers at mmWave frequency could be sensitive to the soldering and circuit elements, and thus, a promising direction to minimize the loss of mmWave rectifiers is to reduce the utilization of surface mounted diode (SMD) devices and chip components, in which the matching, RF filtering, and dc filtering circuit elements should have been transformed purely into printed transmission lines on a highly efficient substrate (e.g., RT5880) with low power loss. In addition, the antenna and rectifier could be codesigned to minimize the insertion loss caused by the impedance matching networks for a wide bandwidth over mmWave spectrums.

Hence, we will consider the development of a codesigned wideband rectenna, for the first time, at the mmWave frequencies with state-of-the-art conversion efficiency.

A. ME Dipole

ME dipole antenna has been demonstrated to have wide impedance bandwidth, wide beamwidth, and reasonably high gain for both microwave and mmWave frequency bands [36], [37], [38], [39]. The complementary radiation originated from electric and magnetic dipoles could form a unidirectional pattern with a wide beamwidth of >100°. Therefore, we will employ the ME dipole in the proposed rectenna design. Different from the conventional ME dipole that only concerns its antenna characteristics, for the proposed rectenna design, the capability for circuit integration with PCB

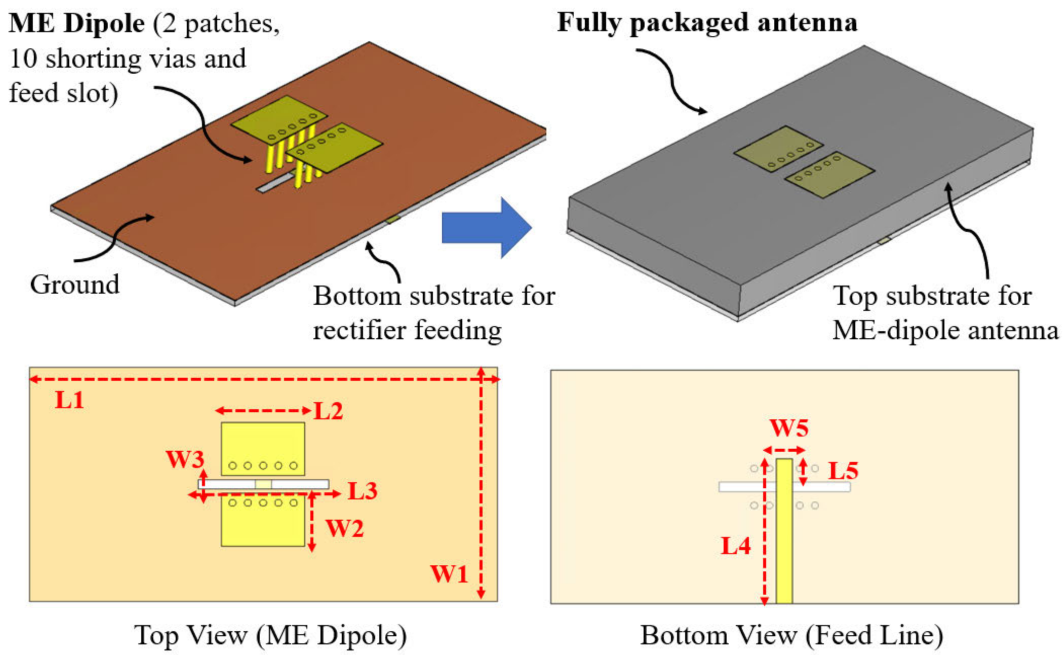

Fig. 3. Proposed wideband mmWave ME dipole for antenna and rectifier codesign. The antenna is produced on high-frequency RT5880 substrate with a thickness of 1.575 mm and the feed line is produced on the same material with a thickness of 0.254 mm, which is attached to the bottom. List of parameters: L1 = 20 mm, W1 = 10 mm, L2 = 3.56 mm, W2 = 2.25 mm, L3 = 5.6 mm, W3 = 0.4 mm, L4 = 6.2 mm, L5 = 1.2 mm, and W5 = 0.7 mm. The via holes are metallized holes with a diameter of 0.3 mm and a gap (center to center) of 0.65 mm.

mmWave rectifier and antenna-to-rectifier codesign will also need to be carefully considered here.

Fig. 3 shows the proposed ME dipole antenna that consists of two patches (electric dipole arm), 2×5 shorting vias, and a feeding slot (magnetic dipole). The electric dipole is hosted by using a single layer of high-frequency RT5880 substrate (dielectric constant = 2.1 and loss tangent = 0.001 at 40 GHz) with a thickness of 1.575 mm. The printed patch dipole arms are linked electrically to the ground via ten shorting pins on both patches, with a metallized hole diameter of 0.3 mm. The detailed dimensions for an optimized design covering 20–32 GHz are given in the caption of Fig. 3. The overall size of the ME dipole is $20 \times 10 \times 1.9$ mm^3. It is noted that since the antenna is aperture fed, a microstrip feed line is printed on a thin layer of RT5880 (thickness = 0.254 mm) and located on the bottom of the antenna. The operating principle of the proposed ME dipole is shown in Fig. 4 where the magnetic dipole is mainly determined by the feed slot. It is slightly different from the probe-fed ME dipole where the electric dipole current does not travel along the shorted patch/vias [40]. While the probe-fed method has shown potential in reducing antenna height [41] and extending bandwidth [42], it is important to note that this approach often requires a more intricate structural design and the incorporation of shorting vias to facilitate the probe connection. This complexity can subsequently pose challenges for the seamless integration of rectifiers at the system level, particularly in the context of mmWave rectennas.

Fig. 5 shows the 3-D/2-D radiation pattern and surface current distribution of the proposed ME dipole at 24 and 30 GHz. It can be seen that the surface current on the top patch and shorting vias flows along the desired current directions of an electric dipole [see Fig. 5(a)], while the surface current around the feeding slot is perpendicular to the electric dipole, thereby forming the magnetic dipole radiation. At phase = 0°, the horizontal current on the planar dipole is dominated where the currents with quasi-sinusoidal distribution on the electric dipoles are found to be maximum. In contrast, at phase = 90°, the horizontal currents and the aperture electric field are minimized, while vertical currents on the shorting pins are strongly excited. The antenna exhibits a unidirectional beam of >90° beamwidth and around 6.3–7.7 dBi gain [e.g., Fig. 5(b)] with a very low backward radiation [see Fig. 5(c)] over the wide frequency band of interest.

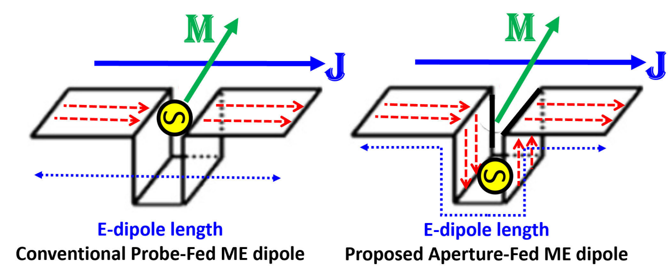

Fig. 4. Operating mechanism comparison between conventional probe-fed ME dipole and the proposed aperture-fed ME dipole. Red dashed line represents the surface current distribution on the electric dipole arm.

For the antenna-to-rectifier codesign, it is crucial to analyze the antenna resonance and impedance, from a circuit point of view. The frequency dependence of the antenna/rectifier complex impedance could play an important role in the conjugate matching for wideband rectifiers if the antenna impedance could be tuned strategically [39], [40]. The simulated complex impedance of the ME dipole is shown in Fig. 6(a) and (b).

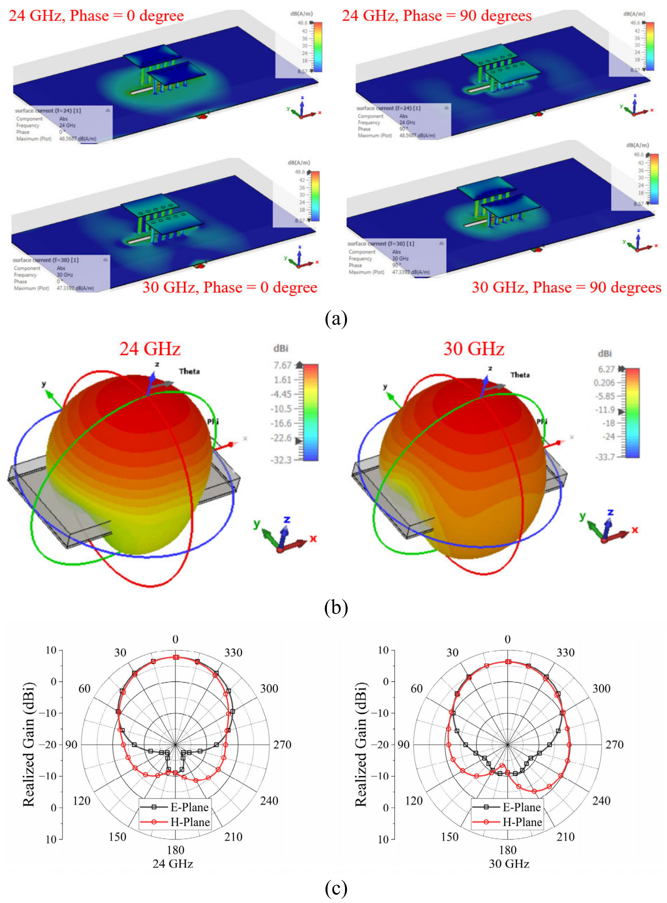

Fig. 5. (a) Surface current distribution, (b) 3-D radiation pattern, and (c) 2-D radiation pattern (over E-plane and H-plane) of the proposed ME dipole antenna at 24 and 30 GHz.

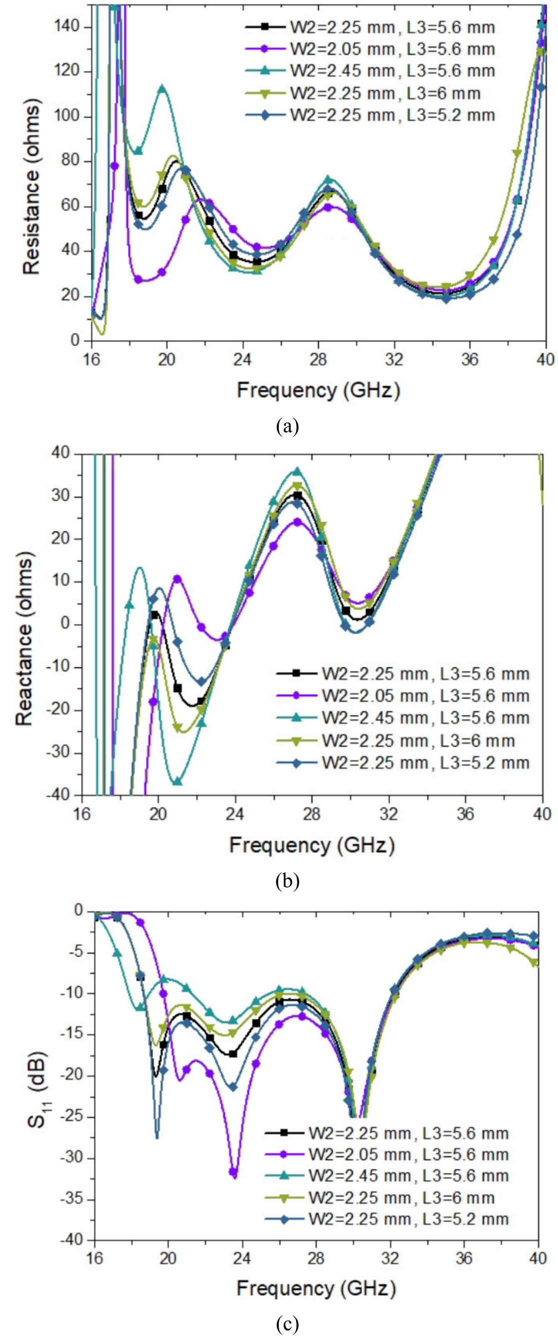

Fig. 6. (a) Read part (resistance) of the antenna impedance. (b) Imaginary part (reactance) of the antenna impedance. (c) Reflection coefficient of the proposed ME dipole antenna for 50-Ω port impedance.

Here, we show examples of tuning two major parameters: W2 (electric dipole length) and L3 (magnetic dipole length). To help readers get a better understanding, the reflection coefficient calculated using 50-Ω port impedance is shown in Fig. 6(c). By adjusting the electric dipole, the antenna impedance varies significantly at around 20 GHz, while the impedance will change at around 24 GHz when the magnetic dipole L3 is tuned. Such a freedom of impedance tuning could contribute to the conjugate impedance matching with nonlinear rectifier over a range of frequencies, powers, and loads [43], [44].

Fig. 6(a)–(c) shows that the proposed ME dipole is capable of achieving a wide impedance bandwidth over 20–32 GHz [fractional bandwidth (FBW) = 46%] for $S_{11} < -10$ dB and has an excellent capability for impedance tuning either inductively or capacitively to match the rectifiers over the aforesaid frequency band. Note that S_{11} in Fig. 6(c) is for illustrative examples only, and it might not be identical to the codesigned rectenna S_{11}, as the impedance of rectifying diode is a complex number and a nonlinear function of frequency, power, and circuit loads.

B. Wideband mmWave Diode and Rectifier

For the mmWave rectifier design, the feed line from the ME dipole antenna could be used to link the rectifier on the printed substrate. Importantly, an accurate diode model becomes crucial to improve the precision and reliability of the overall rectifier/rectenna performance. Some work has considered modeling the mmWave diodes either using the SPICE parameter-based behavior model [30], [47] or using experimental data matrix and real-time S-parameter files [48]. It is generally concluded that the MA4E1317 diode could perform effectively up to 80 GHz with high conversion efficiency (>40%) if the mmWave rectifying circuit is properly designed.

For the diode modeling, here, we employ model parameters of MA4E1317 that are extracted from the $I-V$, $C-V$,

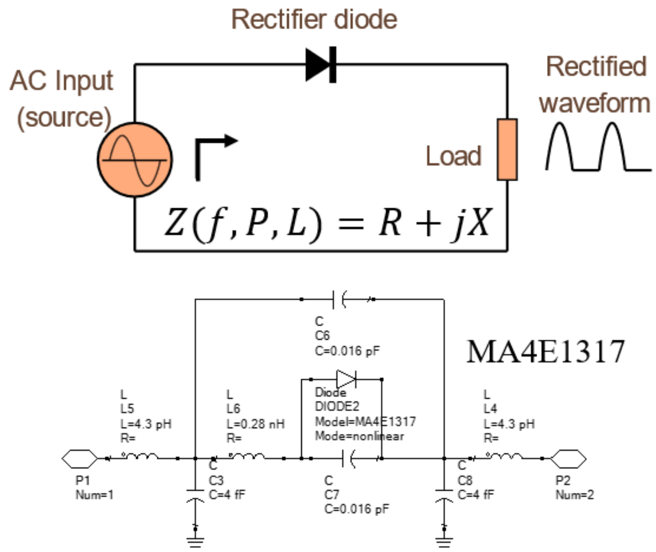

Fig. 7. mmWave diode behavior model and circuit diagram to evaluate its complex impedance variations against frequency, power, and load.

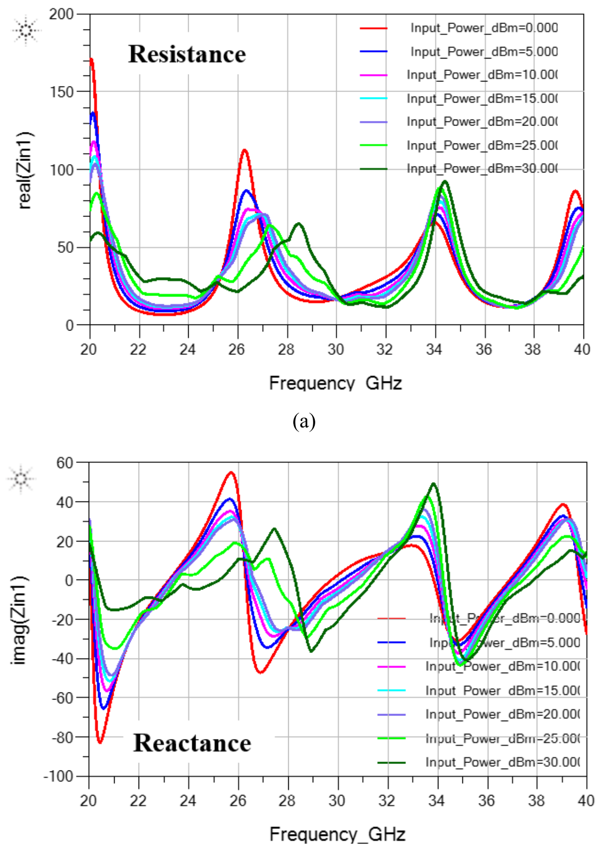

(a)

(b)

Fig. 8. (a) Resistance and (b) reactance of mmWave diode MA4E1317-based single diode rectifier at different powers from 0 to 30 dBm and frequency span from 20 to 40 GHz. The load impedance is 100 Ω.

and small-signal S-parameter measurements, as reported in [48]. Such a diode model is particularly suitable for rectifier design for a large dynamic range in terms of power and frequency. As shown in Fig. 7, the diode mode jointly utilizes the SPICE parameter of MA4E1317 and parasitic elements that are determined by the $I-V$, $C-V$, and small-signal S-parameters.

To analyze the performance of the MA4E1317 diode at the circuit level, we constructed a simple series diode circuit using Advanced Design System (ADS) software, as shown in Fig. 7. We numerically swept the impedance $Z(f, P, L)$ of the rectifier, considering a load of L = 100 Ω, as a function of frequency ranging from 20 to 40 GHz, and as a function of input power ranging from 0 to 30 dBm (representative power levels for wireless charging). The results are presented in Fig. 8.

The diode exhibits several resonances at approximately 26, 34, and 40 GHz. Both the real part (resistance) and the imaginary part (reactance) of the impedance are sensitive to changes in input power, with a variation range and frequency shift of around 15%–20%. Notably, the impedance variation is much more pronounced compared to low-frequency diodes. These results serve as valuable reference data for determining the frequency dependence of the ME dipole antenna impedance, as shown in Fig. 6. By utilizing such impedance curves, we can achieve a codesigned conjugate matching across the wide frequency range of 20–40 GHz.

C. mmWave Rectifier Codesign

The schematic of the proposed rectifier is shown in Fig. 9(a), where the tunable antenna impedance is imported into ADS for the rectifier codesign. The codesign process was conducted in real time, with the antenna impedance being updated immediately by optimizing the CST antenna structures based on the feedback information of the ADS rectifier efficiency and impedance matching performance. In this way, the ADS was utilized to tune the CST antenna impedance for achieving complete matching of the wideband rectenna.

Such a method has been reported in our previous articles [43], [44] as well as in some other articles [45], [46]. However, it is important to note that all these previous studies primarily focused on frequencies below 5 GHz. As the loss of SMD components and rectifying diodes significantly increases at mmWave frequencies, a new design method specifically suitable for mmWave rectenna codesign is necessary. Our work addresses this gap and presents a novel design method that caters to the unique challenges of mmWave frequencies, which has not been previously explored in the literature.

To model the mmWave rectifier, our main objective is to minimize the use of SMD components, high-frequency diodes, and soldering. In our approach, a shunt circuit branch is positioned before the series-connected behavior model of the mmWave diode MA4E1317. Following the diode model, two dc filters (radial stubs) are connected to reject the higher order harmonics at 36 and 48 GHz. This configuration forms a closed-circuit loop, consisting of the shunt branch, diode, dc filters, and load. By applying Kirchhoff's voltage law (KVL), voltage drops can be accounted for, ensuring the generation of a nonzero output voltage with minimal circuit components.

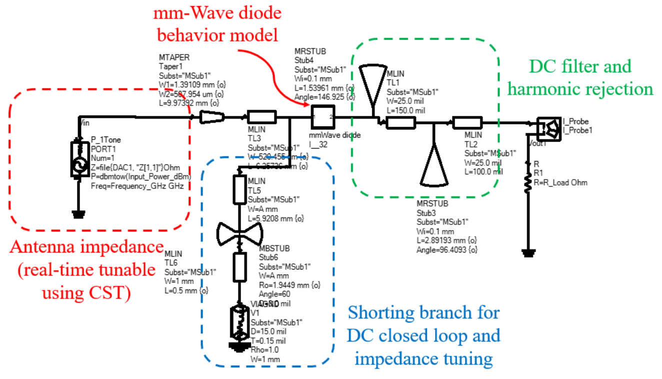

(a)

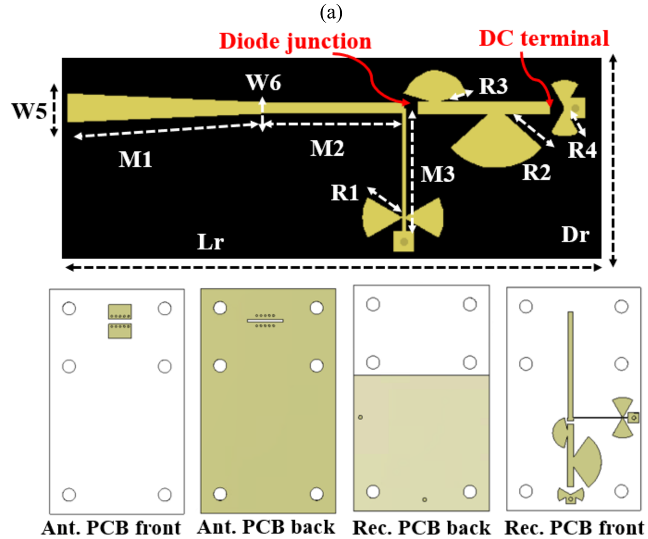

(b)

Fig. 9. (a) Schematic of the codesigned wideband mmWave rectenna. (b) Layout of the proposed mmWave rectifier and PCB layer structure. W5 = 1.4 mm, W6 = 0.5 mm, M1 = 10 mm, M2 = 6.3 mm, M3 = 5.9 mm, R1 = 1.9 mm, R2 = 2.9 mm, R3=1.5 mm, R4 =1.3 mm, Lr = 35 mm, and Dr = 16 mm.

The overall design of the rectifier is kept simple, without the need for a dedicated impedance matching network. Instead, a taper line is employed to smoothly feed the antenna, facilitating the transmission of broadband impedance in the real part. It is important to note that while the shunt circuit branch primarily serves the purpose of a dc closed loop, its contribution to impedance tuning is limited due to its shunt inductance equivalence.

Once the antenna impedance is tuned by adjusting the ME dipole parameters (as shown in Fig. 3), the frequency and power-dependent impedance of the rectifier are updated accordingly to achieve optimal conjugate matching across the wide frequency range [43], [44]. Simultaneously, the rectifier topology undergoes updates to accommodate this dynamic codesign concept. The optimized rectifier topology is shown in Fig. 9(b), and the corresponding dimensions are provided in the captions. Notably, the overall rectifier design is nearly solderless. Only one diode junction and one dc terminal (for the chip resistor) require soldering, effectively minimizing the negative effects associated with multiple soldering points in conventional wideband impedance matching networks and SMD components.

In addition, it is important to mention the presence of two via holes on the rectifier. One via hole is designated for the shunt circuit branch, while the other is for the ground connection of the dc terminal. These holes will be metallized with a gold coating during fabrication to minimize their impact on circuit performance. The utilization of double radial stubs for the mmWave rectifier via holes offers advantages in terms of low loss, high tolerance, and high precision during prototype fabrication [49]. Therefore, these stubs are employed to achieve the ultimate objective of realizing high-efficiency wideband mmWave rectennas with minimal insertion loss.

Compared to existing codesign strategies for low-frequency wideband rectennas, our method provides a unique guideline to effectively mitigate component losses at mmWave frequencies. It achieves this by transforming all necessary circuit components into a printed layout with low loss and high reliability. This approach allows for an elegant reduction in component losses, specifically tailored for the challenges of mmWave frequencies.

The rectifier topology in Fig. 9(b) will be printed on a single-layer, double-sided high-frequency RT5880 substrate with a sheet thickness of 0.254 mm. The overall dimension is just $35 \times 16 \times 0.254$ mm^3. An example of stacking the ME dipole antenna on top of the rectifier is also shown in the figure where the rectifier and antenna share the same ground plane, which is sandwiched in the middle. Having optimized the codesigned rectenna, the simulated S_{11} and the RF-to-dc conversion of the proposed mmWave rectenna are shown in Fig. 10(a) and (b). It is worth noting here that the calculation of S_{11} utilizes the complex impedance of the ME dipole antenna and rectifiers, rather than the conventional 50-Ω impedance. Our investigation into the frequency dependence within the range of 20–40 GHz has revealed that the rectenna exhibits relatively good impedance matching over the 24–34-GHz range. Moreover, we have achieved a conversion efficiency of up to 67% when the input power level is 20 dBm. The average conversion efficiency across the wide bandwidth is >30%, 40%, 50%, and 55% for input power levels at 5, 10, 15, and 20 dBm, respectively.

Please note that the presented conversion efficiency is calculated using a load resistance of 100 Ω and using the following formula:

$$\eta_{RF-DC} = \frac{V_{DC}^2}{R_L \times P_{RF}} \tag{1}$$

where P_{RF} is the received RF power by the antenna, or in other words, the input RF power to the rectifier V_{DC} is the output voltage and $R_L = 100$ Ω. In addition, the power dependence of the rectifier performance is analyzed at three different frequencies (24, 29, and 34 GHz) and shown in Fig. 11.

The optimal input power range for this rectenna is around 0–27 dBm in which S_{11} is less than −9 dB for matching.

In terms of the power-dependent conversion efficiency, the proposed rectenna has a peak efficiency of around 50%–65% at around 20-dBm power at different frequencies, and the efficiency nearly drops to 0 at the input power of −10 dBm. In summary, the proposed wideband rectenna can indeed perform well for a wide FBW of 34.5% (24–34 GHz)

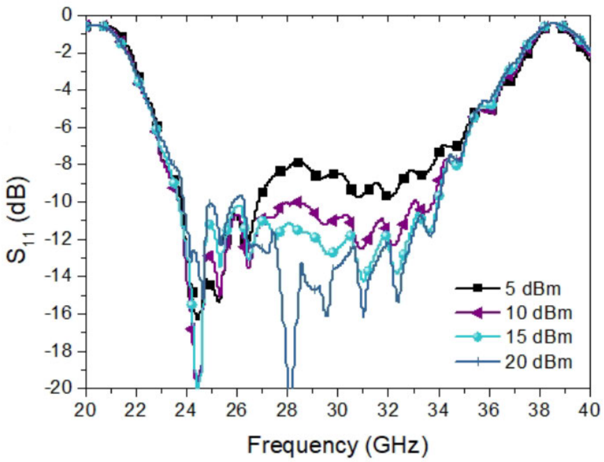

(a)

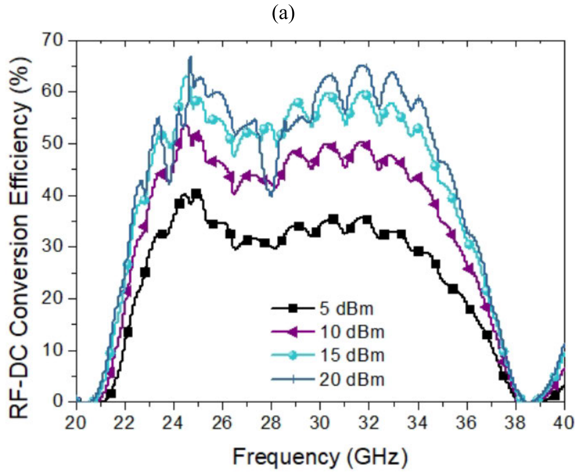

(b)

Fig. 10. (a) Reflection coefficient of the codesigned rectenna versus frequency at three power levels. The reflection coefficient is calculated using the complex impedance of antenna and rectifiers. (b) RF-to-dc conversion efficiency of the proposed wideband mmWave rectenna versus frequency at three power levels.

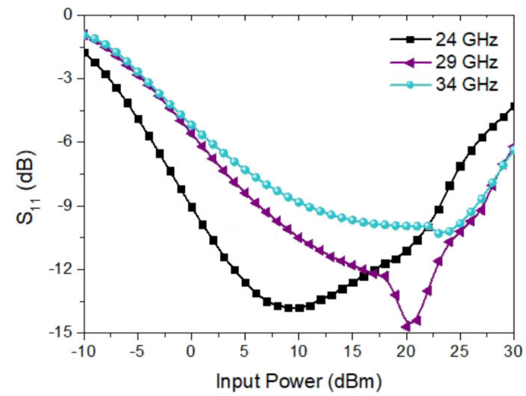

(a)

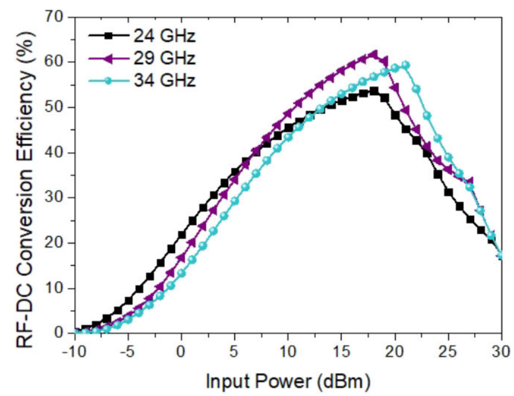

(b)

Fig. 11. (a) Reflection coefficient of the codesigned rectenna versus power at three frequencies. (b) RF-to-dc conversion efficiency of the proposed wideband mmWave rectenna versus power at three frequencies.

with RF-to-dc conversion efficiency above 50% for power >15 dBm and a rectifiable power range of 5–27 dBm (efficiency around 30%–60%).

IV. Fabrication and Measurement

The proposed rectenna was fabricated using high-precision laser PCB etching technology. The prototype is shown in Fig. 12(a), illustrating the front and back sides of the device. The ME dipole, which plays a crucial role in the rectenna, is highlighted within a 20 × 10 mm area. The backside of the ME dipole is fully metallized, except for a centralized slot for rectifier feeding. The rectifier itself was printed on a double-sided PCB, and its placement did not interfere with the overlapping region of the top ME dipole. In this region, the ground metal was removed to allow for feed line cointegration. The assembly of the entire rectenna was achieved without the need for soldering or gluing. Instead, six air holes were drilled along the PCB edges, and nylon screws were tightly fit into these holes to secure the components, as shown in Fig. 12(a).

To ensure the proper flow of dc current and maintain the rectifier's performance and load impedance, the dc wires were soldered after the rectifying diodes and dc pass filters.

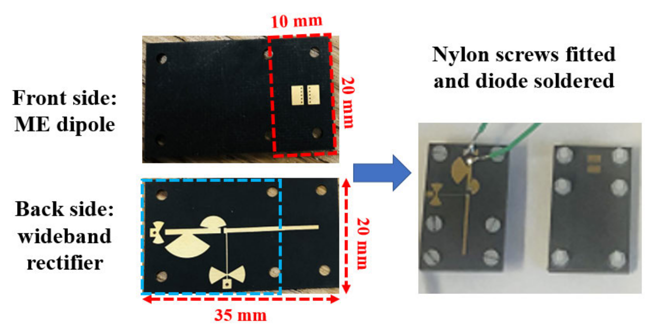

(a)

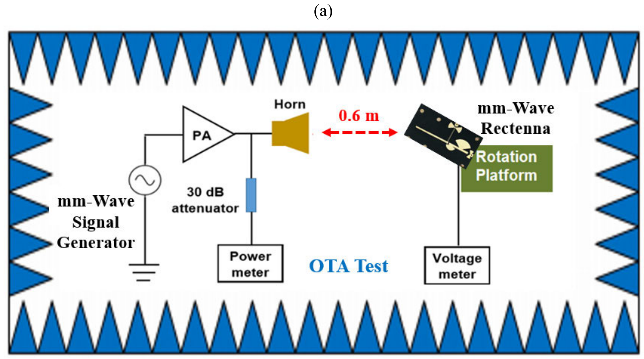

(b)

Fig. 12. (a) Fabricated prototype of the proposed mmWave rectenna. (b) Measurement setup for OTA test of the rectenna within an anechoic chamber.

This configuration only permits the passage of dc current through the wires, without affecting the RF performance of the rectifier. During the measurement process, we compared the results obtained using both dc wires and dc probes and found that they yielded identical performance.

The measurement setup of the rectenna is shown in Fig. 12(b). A wideband mmWave signal generator N5183B was used to generate the signal from 20 to 40 GHz, which was then amplified by a 10-W monolithic microwave integrated circuit (MMIC) wideband mmWave PA QPA2640D manufactured by Qorvo. The signal was transmitted through high gain 18–40-GHz horn antenna HA40G and was measured by using a power meter (spectrum analyzer) and a 30-dB attenuator. The rectenna was tested over-the-air (OTA) at a 0.6-m distance to the horn inside an anechoic chamber, where the broadside direction of the ME dipole was targeted toward the horn. The received power by the rectenna can be calculated using

$$P_r = P_t + G_t + G_r + 20\log_{10}\frac{\lambda}{4\pi D} \tag{2}$$

where P_r is the input RF power to the rectifier in dBm, P_t is the transmitting power of the horn in dBm, G_t is the realized gain of the horn in dBi, Gr is the realized gain of the proposed rectenna in dBi, λ is the wavelength of interest, and D is the distance ($D = 0.6$ m). Here, the realized gain (ME dipole directivity $\times$ rectenna matching efficiency) of the rectenna was used and therefore might be not perfectly accurate. However, such a method has shown good result consistency and accuracy in such integrated rectenna design in our previous work [43], [44] and other published articles [29], [31]. Indeed, validating conjugate matching experimentally is complex, as conventional methods fall short. In our experimental setup, both antenna and rectifier underwent testing, assessing S-parameters with 50-Ω SMA connectors. This method gauges impedance on the Smith chart, scrutinizing fabrication accuracy. We cross-validated simulation outcomes via 50-Ω SMAs, accounting for fabrication and diode model uncertainties. Although direct matching efficiency testing is challenging, separate experiments authenticate antenna and rectifier impedance, enabling optimized consistency. By adjusting the transmitting power, the received power can be maintained at a constant level over the wide frequency range. A comparison between the simulated and measured frequency dependence of RF-to-dc conversion efficiency is shown in Fig. 13(a). The results are compared at 10- and 15-dBm received power levels, which show that the proposed rectenna can indeed realize very high conversion efficiency over the frequency band of interest. Moreover, the power dependence of the conversion efficiency is compared at 26, 29, and 33 GHz [see Fig. 13(b)]. The consistency between simulated and measured results is generally good, but we have just measured up to the power level of 24 dBm, due to the limits of saturation power (<10 W) of the mmWave PA.

Furthermore, to assess the performance of the rectenna, we placed it on a rotational platform inside the chamber. The received dc voltage was recorded at different Theta and Phi angles, with the antenna broadside as the reference. The normalized dc voltage pattern, obtained with a received power of 15 dBm and a maximum dc voltage of 1.42 V, is shown in Fig. 13(c). The pattern demonstrates that the proposed rectenna exhibits a relatively wide beamwidth, spanning over 90°. It is important to note that the dc voltage pattern of the rectenna may slightly differ from the ME dipole radiation pattern due to the nonlinear rectifier and circuit loads [50]. To explore the impact of load resistance, we measured the proposed rectenna at a fixed input power of 15 dBm while varying the load resistance from 10 to 900 Ω. The results are presented in Fig. 14. It was observed that the peak efficiency occurred at a load resistance of 100 Ω, and the optimal load range for achieving an efficiency greater than 50% was approximately between 50 and 350 Ω. The validity of this load range was verified at two different frequencies, specifically 29 and 31 GHz.

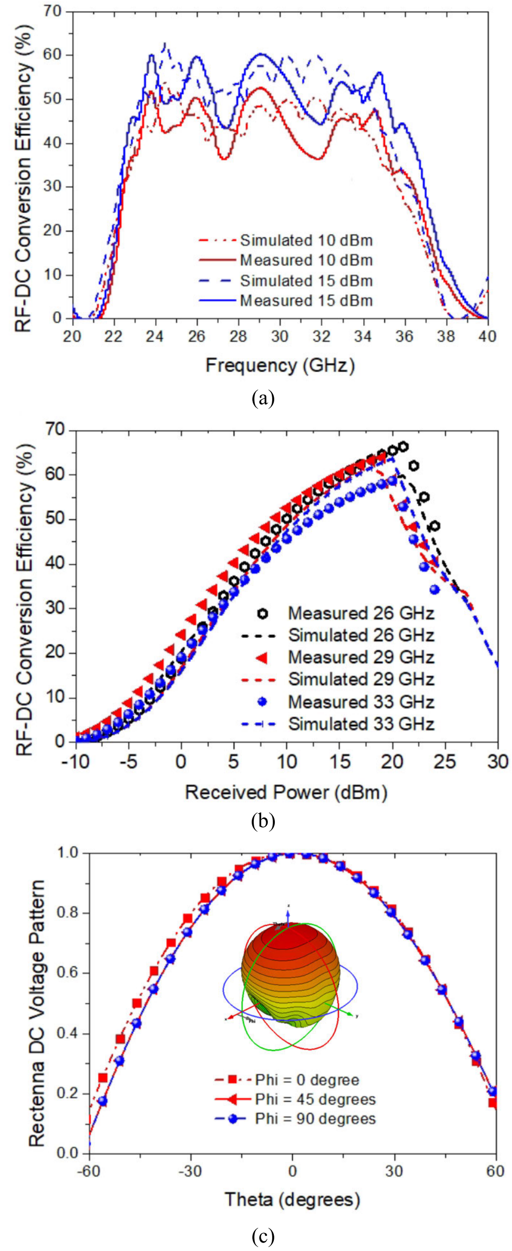

Fig. 13. Experimental results of the proposed rectenna for (a) RF-to-dc conversion efficiency versus frequency, (b) RF-to-dc conversion efficiency versus power, and (c) normalized dc voltage pattern of the rectenna at different cutting angles.

TABLE I
COMPARISON OF THE PROPOSED WIDEBAND MM-WAVE RECTENNA AND RELATED DESIGNS

Ref. (year)	Impedance bandwidth (GHz)	FBW*	Need impedance matching	Overall complexity	Overall dimension of the complete rectenna	Maximum conversion efficiency	Rectenna overall gain and half power beamwidth
[25] (2020)	20 – 26.5	28%	Yes	Medium	32.6 mm × 16 mm × 0.3 mm	12% at 10 dBm	~8 dBi and ~50 degrees (single antenna + rectifier)
[29] (2014)	23.5 – 25.2	6.9%	Yes	Complex	55 mm × 50 mm × 1.8 mm	40% at 20 dBm	~12.6 dBi and ~40 degrees (antenna array + rectifier)
[31] (2021)	34.5 – 35.5	3%	Yes	Complex	32 mm × 128 mm × 1 mm	60.9% at 19 dBm	~14.7 dBi and ~30 degrees (antenna array + rectifier)
This work (2022)	**24 – 34.5**	**36%**	**No**	**Simplest**	**35 mm × 20 mm × 1.9 mm**	**67% at 20 dBm**	~8 dBi and ~90 degrees (single antenna + rectifier)

*FBW: Factional Bandwidth

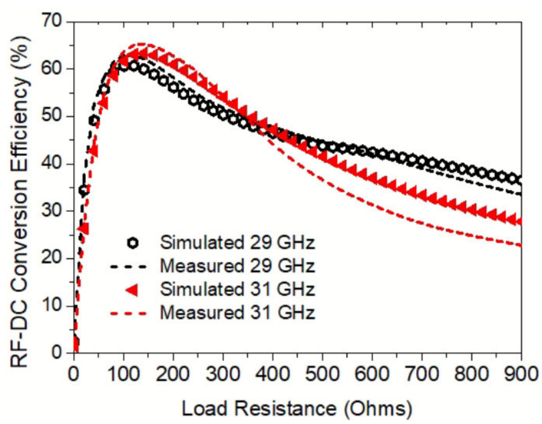

Fig. 14. Comparison between simulated and measured RF-to-dc conversion efficiency versus load resistance. The input power is fixed at 15 dBm during the experiment.

The proposed rectenna has been compared with state-of-the-art mmWave rectennas in terms of either wideband capability or high efficiency (see Table I). The comparison highlights the unique features and advantages of our design. The comparison clearly demonstrates that our work achieves a significant enhancement in RF-to-dc conversion efficiency across a wide mmWave spectrum. This improvement is attributed to the codesigned structure, which enables lossless impedance matching and minimizes the negative effects of soldering on circuit performance. Compared to a single wideband antenna-based rectenna design [25], our efficiency is 40% higher, due to the utilization of a low-loss substrate and a novel integration method. In addition, our design offers a broader beamwidth due to the wide-beam nature of the ME dipole. When compared to antenna array-based designs [29], [31], our design excels in terms of reduced physical size while maintaining high efficiency. In summary, our design showcases compactness, wide beamwidth, and commendable gain.

V. MULTINODE CHARGING AND TRACKING

Unlike traditional radar (RDA) and phased array radar (TR) technologies, the wireless power transmitter based on LWA does not require complex antenna arrays, phase shifters, signal mixers, or active semiconductor switches. Instead, beamforming is achieved through software-controlled

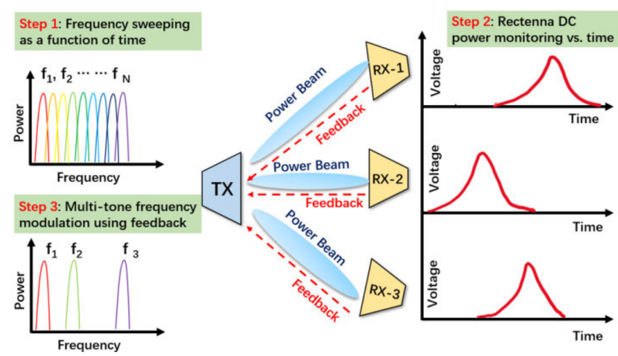

(a)

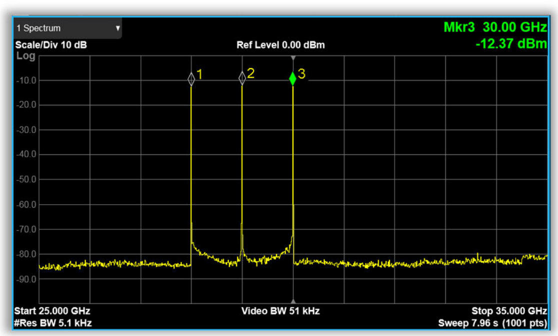

(b)

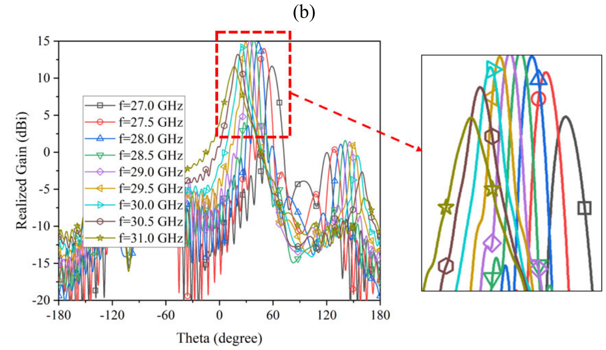

(c)

Fig. 15. (a) Proposed concept for multinode wireless charging and tracking using the proposed WPT system. (b) Example of the multitone spectrum for mmWave modulation. (c) Beam scanning radiation pattern of the proposed LWA prototype [51].

frequency modulation. This approach offers a simplified node tracking mechanism. To perform node tracking, the transmitter sweeps the frequency of the transmitting (TX) signal at a known rate over a defined time period. Concurrently, the dc power received from the RX rectenna node is continuously monitored in real time, synchronized with the transmitter's frequency sweeping. When the peak dc output is detected, the receiver sends a beacon signal back to the transmitter, indicating the optimal time instance for beamforming at a specific TX signal frequency. This enables precise localization of the optimal frequency for beamforming.

Furthermore, our design allows for multitarget moving node tracking by utilizing multitone frequency modulation and sweeping, as shown in Fig. 15(a). The LWA, as shown in Fig. 15, exhibits unique beam shapes that vary with its operating frequency. This results in a scanning beam characteristic, offering a distinct advantage over conventional phased array scanning methods. In conventional approaches, beam scanning is achieved by manipulating the phase of antenna elements using phase shifters while keeping the frequency constant. In our work, we can achieve beam scanning simply by changing the input signal's frequency, which can be easily controlled through software using the signal generator.

Here, we show an example of charging three different nodes simultaneously. The waveform for the frequency modulation is given in Fig. 15(b), which shows a three-tone continuous waveform (CW) signal at 28, 29, and 30 GHz. The frequency tones could either be controlled using a time-switching fashion or be excited at the same time, dependent on the number of receiving nodes and total TX power. An LWA prototype covering 27–31 GHz was employed to transmit the signal, where the frequency-dependent beam-scanning patterns of the LWA are shown in Fig. 15(c). It can be seen that the LWA could realize a 50° beam scanning range over 27–31 GHz, where the radiating angles for 28, 29, and 30 GHz are around Theta = 15°, 30°, and 45°, respectively [51]. In this work, the scanning range for a 1-dB gain drop spans from 23.5° to 50° (with a frequency range of 27.5–30.2 GHz), while the 3-dB gain scanning range extends from 17° to 58.5° (across a frequency range of 27–30.9 GHz).

The experimental system of the proposed mmWave multinode charging and tracking is shown in Fig. 16(a), which consists of prototypes for LWA, PA, proposed rectennas, load, node dc sensor, and bluetooth low energy (BLE) gateway for feedback control. The dc sensor was developed using a low-cost programmable sensor platform (CYALKIT-E02 BLE Sensor Beacon), which has been reported in our previous work [52]. The rectenna dc peak versus time instance could be transmitted to the gateway and to identify the optimal frequency over the scanning frequency for TX. The scanning rate was 100 MHz per 500 μs over 28–30 GHz, configured within the signal source. An example of the three-node simultaneous charging scenario is shown in Fig. 16(b), where rectenna nodes 1–3 were positioned at a 1-m distance from the LWA transmitter. These rectennas were situated within the far-field beam angles of 15°, 30°, and 45°. Within this range,

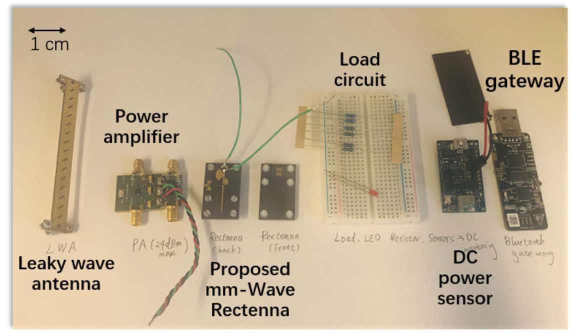

(a)

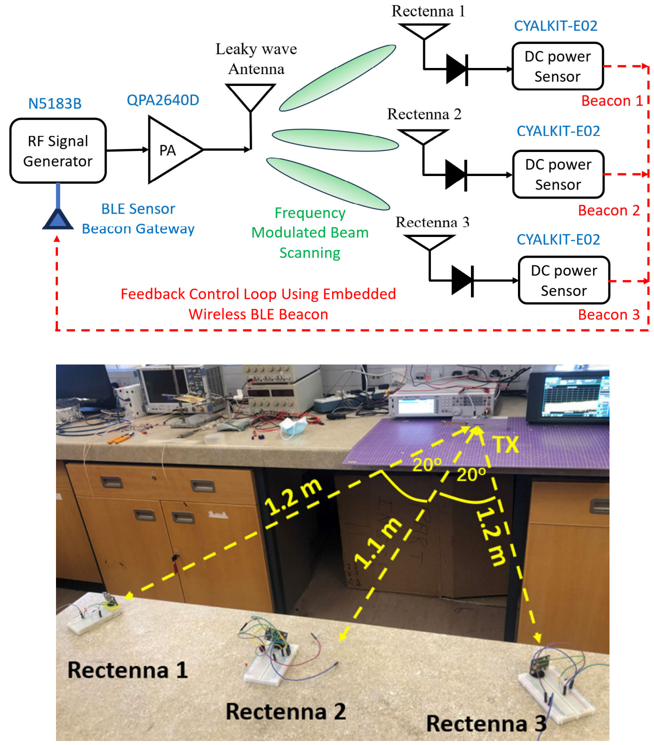

(b)

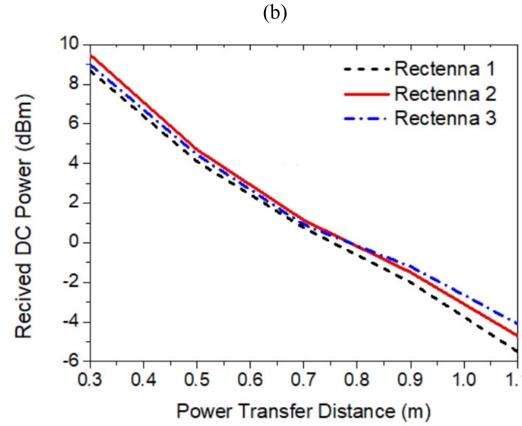

(c)

Fig. 16. (a) Prototypes and assembly for the proposed WPT system. (b) Example picture and system layout for wireless powering three rectenna nodes with feedback loop control. (c) Receiving rectenna node dc power versus distance for transmitting EIRP of 55 dBm.

bean scanning gain reduction is minimal—less than 1 dB, as evidenced in Fig. 15(c). Unlike standard antenna arrays, the coupling dynamics of rectenna arrays are distinct, as RF signals are rectified into dc under optimal matching conditions. This underscores the adequacy of a half-wavelength separation for rectenna array spacing. The EIRP was set at 55 dBm. By harnessing the multitone spectrum shown in Fig. 15(b), the three receiving nodes can be efficiently powered wirelessly. The measured dc power output from the three nodes, plotted against the power transfer distance, is shown in Fig. 16(c). It can be seen that rectenna 2 has a bit higher power compared to rectennas 1 and 3. This was probably due to the slight gain drop of the LWA at 28 and 30 GHz, compared to its highest gain at 29 GHz (around 15 dBi).

We would like to emphasize that the proposed WPT system is preliminary research, and it is the first time to showcase multitarget charging using mmWave power. There is still plenty of room for further investigations, for example: 1) the adaptive dc control for PA to mitigate the gain diversity of different frequencies; 2) fast feedback control for moving targets; and 3) a more effective LWA transmitter with higher gain, smaller size, and wide scanning angles over limited spectrums. In comparison to our previous conference contribution in [53], which provided a brief introduction to the overall system structure and emphasized the significance of wideband mmWave rectenna design, this article substantially delves into the technical intricacies of mmWave rectenna codesign. It comprehensively covers various aspects, such as diode modeling, antenna impedance optimization, rectifier cosimulation, and the underlying physics behind all simulation and experimental results. Furthermore, this article incorporates an extensive set of experimental results to demonstrate the feasibility of mmWave WPT and to quantify the performance of the novel mmWave wideband rectenna.

VI. Conclusion

In this article, we have presented a codesign strategy for mmWave rectennas, enabling them to cover a wide frequency bandwidth (>36%) while achieving high RF-to-dc conversion efficiency (>50%, up to 67%). Our approach involves combining an ME dipole with high-frequency MA4E1317 diodes, allowing for efficient antenna-to-rectifier impedance matching without the need for transmission line components at the circuit level. The proposed rectenna offers several advantages, including wide bandwidth, wide beamwidth, and improved efficiency at mmWave frequencies. Furthermore, we demonstrate the practical application of the proposed rectenna in a multinode simultaneous wireless charging system. Our preliminary results showcase the feasibility of passive beamforming using multitone frequency-modulated LWA transmitters to power three wideband rectenna nodes.

Moving forward, our future work will focus on feedback control and moving target tracking using the proposed rectenna and WPT system. These advancements hold great potential for enhancing the capabilities and efficiency of mmWave beamformed wireless charging. As the first demonstration of passive mmWave beamformed wireless charging, our work has significant implications for both the academic and commercial wireless power research community.

References

[1] B. Strassner and K. Chang, "Microwave power transmission: Historical milestones and system components," *Proc. IEEE*, vol. 101, no. 6, pp. 1379–1396, Jun. 2013.

[2] G. A. Covic and J. T. Boys, "Inductive power transfer," *Proc. IEEE*, vol. 101, no. 6, pp. 1276–1289, Jun. 2013.

[3] J. S. Ho, S. Kim, and A. S. Y. Poon, "Midfield wireless powering for implantable systems," *Proc. IEEE*, vol. 101, no. 6, pp. 1369–1378, Jun. 2013.

[4] A. Costanzo et al., "Electromagnetic energy harvesting and wireless power transmission: A unified approach," *Proc. IEEE*, vol. 102, no. 11, pp. 1692–1711, Nov. 2014.

[5] C. Song et al., "Advances in wirelessly powered backscatter communications: From antenna/RF circuitry design to printed flexible electronics," *Proc. IEEE*, vol. 110, no. 1, pp. 171–192, Jan. 2022.

[6] S. Assawaworrarit, X. Yu, and S. Fan, "Robust wireless power transfer using a nonlinear parity-time-symmetric circuit," *Nature*, vol. 546, pp. 387–390, Jun. 2017.

[7] S. Y. Hui, "Planar wireless charging technology for portable electronic products and qi," *Proc. IEEE*, vol. 101, no. 6, pp. 1290–1301, Jun. 2013.

[8] A. Kurs, A. Karalis, R. Moffatt, J. D. Joannopoulos, P. Fisher, and M. Soljacic, "Wireless power transfer via strongly coupled magnetic resonances," *Science*, vol. 317, no. 5834, pp. 83–86, Jul. 2007.

[9] A. P. Sample, D. T. Meyer, and J. R. Smith, "Analysis, experimental results, and range adaptation of magnetically coupled resonators for wireless power transfer," *IEEE Trans. Ind. Electron.*, vol. 58, no. 2, pp. 544–554, Feb. 2011.

[10] P. Jaffe and J. McSpadden, "Energy conversion and transmission modules for space solar power," *Proc. IEEE*, vol. 101, no. 6, pp. 1424–1437, Jun. 2013.

[11] S. Kawasaki, "Microwave WPT to a rover using active integrated phased array antennas," in *Proc. 5th Eur. Conf. Antennas Propag. (EUCAP)*, Apr. 2011, pp. 3909–3912.

[12] J. H. Park, D. I. Kim, and K. W. Choi, "Analysis and experiment on multi-antenna-to-multi-antenna RF wireless power transfer," *IEEE Access*, vol. 9, pp. 2018–2031, 2021.

[13] D. Masotti, A. Costanzo, M. Del Prete, and V. Rizzoli, "Time-modulation of linear arrays for real-time reconfigurable wireless power transmission," *IEEE Trans. Microw. Theory Techn.*, vol. 64, no. 2, pp. 331–342, Feb. 2016.

[14] B. Yang, X. Chen, J. Chu, T. Mitani, and N. Shinohara, "A 5.8-GHz phased array system using power-variable phase-controlled magnetrons for wireless power transfer," *IEEE Trans. Microw. Theory Techn.*, vol. 68, no. 11, pp. 4951–4959, Nov. 2020.

[15] H.-Y. Zhang, F.-S. Zhang, F. Zhang, F.-K. Sun, and G.-J. Xie, "High-power array antenna based on phase-adjustable array element for wireless power transmission," *IEEE Antennas Wireless Propag. Lett.*, vol. 16, pp. 2249–2253, 2017.

[16] J. Han et al., "Adaptively smart wireless power transfer using 2-bit programmable metasurface," *IEEE Trans. Ind. Electron.*, vol. 69, no. 8, pp. 8524–8534, Aug. 2022.

[17] S. Yu, H. Liu, and L. Li, "Design of near-field focused metasurface for high-efficient wireless power transfer with multifocus characteristics," *IEEE Trans. Ind. Electron.*, vol. 66, no. 5, pp. 3993–4002, May 2019.

[18] R. González Ayestarán, G. León, M. R. Pino, and P. Nepa, "Wireless power transfer through simultaneous near-field focusing and far-field synthesis," *IEEE Trans. Antennas Propag.*, vol. 67, no. 8, pp. 5623–5633, Aug. 2019.

[19] Y.-Q. Yang, H. Wang, and Y.-X. Guo, "A time-modulated array with digitally preprocessed rectangular pulses for wireless power transmission," *IEEE Trans. Antennas Propag.*, vol. 68, no. 4, pp. 3283–3288, Apr. 2020.

[20] P. D. Hilario Re, S. K. Podilchak, S. A. Rotenberg, G. Goussetis, and J. Lee, "Circularly polarized retrodirective antenna array for wireless power transmission," *IEEE Trans. Antennas Propag.*, vol. 68, no. 4, pp. 2743–2752, Apr. 2020.

[21] H. S. Park and S. K. Hong, "Investigation of time-reversal based far-field wireless power transfer from antenna array in a complex environment," *IEEE Access*, vol. 8, pp. 66517–66528, 2020.

[22] Z.-H. Cheng et al., "Selectively powering multiple small-size devices spaced at diffraction limited distance with point-focused electromagnetic waves," *IEEE Trans. Ind. Electron.*, vol. 69, no. 12, pp. 13696–13705, Dec. 2022.

[23] S. Mizojiri and K. Shimamura, "Wireless power transfer via subterahertz-wave," *Appl. Sci.*, vol. 8, no. 12, p. 2653, Dec. 2018.

[24] D. Surender, Md. A. Halimi, T. Khan, F. A. Talukdar, and S. R. Rengarajan, "5G/millimeter-wave rectenna systems for radio-frequency energy harvesting/wireless power transmission applications: An overview," *IEEE Antennas Propag. Mag.*, vol. 65, no. 3, pp. 2–21, Jun. 2022.

[25] M. Wagih, G. S. Hilton, A. S. Weddell, and S. Beeby, "Broadband millimeter-wave textile-based flexible rectenna for wearable energy harvesting," *IEEE Trans. Microw. Theory Techn.*, vol. 68, no. 11, pp. 4960–4972, Nov. 2020.

[26] A. Eid, J. G. D. Hester, and M. M. Tentzeris, "5G as a wireless power grid," *Sci. Rep.*, vol. 11, no. 1, pp. 1–9, Jan. 2021.

[27] H. Mei, X. Yang, B. Han, and G. Tan, "High-efficiency microstrip rectenna for microwave power transmission at Ka band with low cost," *IET Microw., Antennas Propag.*, vol. 10, no. 15, pp. 1648–1655, Dec. 2016.

[28] A. Takacs, H. Aubert, S. Fredon, L. Despoisse, and H. Blondeaux, "Microwave power harvesting for satellite health monitoring," *IEEE Trans. Microw. Theory Techn.*, vol. 62, no. 4, pp. 1090–1098, Apr. 2014.

[29] S. Ladan, A. B. Guntupalli, and K. Wu, "A high-efficiency 24 GHz rectenna development towards millimeter-wave energy harvesting and wireless power transmission," *IEEE Trans. Circuits Syst. I, Reg. Papers*, vol. 61, no. 12, pp. 3358–3366, Dec. 2014.

[30] S. Ladan and K. Wu, "Nonlinear modeling and harmonic recycling of millimeter-wave rectifier circuit," *IEEE Trans. Microw. Theory Techn.*, vol. 63, no. 3, pp. 937–944, Mar. 2015.

[31] Y. Wang, X.-X. Yang, G.-N. Tan, and S. Gao, "Study on millimeter-wave SIW rectenna and arrays with high conversion efficiency," *IEEE Trans. Antennas Propag.*, vol. 69, no. 9, pp. 5503–5511, Sep. 2021.

[32] Y. Huang, *Antennas: From Theory to Practice*, 2nd ed. Chichester, U.K.: Wiley, 2021.

[33] M. Wagih, A. S. Weddell, and S. Beeby, "Millimeter-wave power harvesting: A review," *IEEE Open J. Antennas Propag.*, vol. 1, pp. 560–578, 2020.

[34] A. A. Oliner and D. R. Jackson, "Leaky-wave antennas," in *Antenna Engineering Handbook*. New York, NY, USA: McGraw-Hill, 2007.

[35] X. Li, J. Wang, G. Goussetis, and L. Wang, "Circularly polarized high gain leaky-wave antenna for CubeSat communication," *IEEE Trans. Antennas Propag.*, vol. 70, no. 9, pp. 7612–7624, Sep. 2022.

[36] Q. Xue, S. W. Liao, and J. H. Xu, "A differentially-driven dual-polarized magneto-electric dipole antenna," *IEEE Trans. Antennas Propag.*, vol. 61, no. 1, pp. 425–430, Jan. 2013.

[37] J. Wang, Y. Li, L. Ge, J. Wang, and K.-M. Luk, "A 60 GHz horizontally polarized magnetoelectric dipole antenna array with 2-D multibeam endfire radiation," *IEEE Trans. Antennas Propag.*, vol. 65, no. 11, pp. 5837–5845, Nov. 2017.

[38] J. Zeng and K.-M. Luk, "Wideband millimeter-wave end-fire magneto-electric dipole antenna with microstrip-line feed," *IEEE Trans. Antennas Propag.*, vol. 68, no. 4, pp. 2658–2665, Apr. 2020.

[39] X. Dai, G.-B. Wu, and K.-M. Luk, "A wideband circularly polarized transmitarray antenna for millimeter-wave applications," *IEEE Trans. Antennas Propag.*, vol. 71, no. 2, pp. 1889–1894, Feb. 2023.

[40] C. Song, E. L. Bennett, J. Xiao, and Y. Huang, "Multimode hybrid antennas using liquid dielectric resonator and magneto-electric dipole," *IEEE Trans. Antennas Propag.*, vol. 69, no. 6, pp. 3132–3143, Jun. 2021.

[41] H. W. Lai and H. Wong, "Substrate integrated magneto-electric dipole antenna for 5G Wi-Fi," *IEEE Trans. Antennas Propag.*, vol. 63, no. 2, pp. 870–874, Feb. 2015.

[42] K. Kang, Y. Shi, and C.-H. Liang, "Substrate integrated magneto-electric dipole for UWB application," *IEEE Antennas Wireless Propag. Lett.*, vol. 16, pp. 948–951, 2017.

[43] C. Song et al., "Matching network elimination in broadband rectennas for high-efficiency wireless power transfer and energy harvesting," *IEEE Trans. Ind. Electron.*, vol. 64, no. 5, pp. 3950–3961, May 2017.

[44] C. Song, Y. Huang, P. Carter, J. Zhou, S. D. Joseph, and G. Li, "Novel compact and broadband frequency-selectable rectennas for a wide input-power and load impedance range," *IEEE Trans. Antennas Propag.*, vol. 66, no. 7, pp. 3306–3316, Jul. 2018.

[45] A. Lopez-Yela and D. Segovia-Vargas, "A triple-band bow-tie rectenna for RF energy harvesting without matching network," in *Proc. IEEE Wireless Power Transf. Conf. (WPTC)*, May 2017, pp. 1–4.

[46] T. S. Almoneef, "Design of a rectenna array without a matching network," *IEEE Access*, vol. 8, pp. 109071–109079, 2020.

[47] S.-P. Gao, W. Hu, H. Zhang, and Y. Guo, "Millimeter-wave rectifiers using proprietary Schottky diodes: Diode modeling and rectifier analysis," in *Proc. Wireless Power Week (WPW)*, Jul. 2022, pp. 180–184.

[48] Q. Chen, X. Chen, H. Cai, and F. Chen, "A waveguide-fed 35-GHz rectifier with high conversion efficiency," *IEEE Microw. Wireless Compon. Lett.*, vol. 30, no. 3, pp. 296–299, Mar. 2020.

[49] S. Ladan, S. Hemour, and K. Wu, "A millimeter-wave wideband microstrip RF and DC grounding," in *Proc. 42nd Eur. Microw. Conf.*, Oct. 2012, pp. 13–16.

[50] T. Q. V. Hoang, E. Séguenot, F. Ferrero, J.-L. Dubard, P. Brachat, and J.-L. Desvilles, "3D voltage pattern measurement of a 2.45 GHz rectenna," *IEEE Trans. Antennas Propag.*, vol. 61, no. 6, pp. 3354–3356, Jun. 2013.

[51] X. Li, L. Wang, J. Wang, and G. Goussetis, "Conformal high gain aperture antenna based on leaky-wave array for CubeSat communication," in *Proc. Int. Symp. Antennas Propag. (ISAP)*, Jan. 2021, pp. 499–500.

[52] C. Song, P. Lu, and S. Shen, "Highly efficient omnidirectional integrated multiband wireless energy harvesters for compact sensor nodes of Internet-of-Things," *IEEE Trans. Ind. Electron.*, vol. 68, no. 9, pp. 8128–8140, Sep. 2021.

[53] C. Song, L. Wang, Z. Chen, G. Goussetis, G. A. E. Vandenbosch, and Y. Huang, "Wideband mmWave wireless power transfer: Theory, design and experiments," in *Proc. 17th Eur. Conf. Antennas Propag. (EuCAP)*, Florence, Italy, Mar. 2023, pp. 1–5.

Chaoyun Song (Senior Member, IEEE) received the B.Eng., M.Sc., and Ph.D. degrees in electrical engineering and electronics from the University of Liverpool (UoL), Liverpool, U.K., in 2012, 2013, and 2017, respectively.

He was an Assistant Professor with the School of Engineering and Physical Sciences (EPS), Heriot-Watt University, Edinburgh, Scotland, U.K. He is currently an Associate Professor (Senior Lecturer) with the Department of Engineering, King's College London, London, U.K. He has published more than 110 papers (including 45 IEEE transactions) in peer-reviewed journals and conference proceedings. His current research interests include wireless energy harvesting and power transfer, rectifying antennas (rectennas), flexible and stretchable electronics, metamaterials and metasurface, and low-power sensors.

Dr. Song was a recipient of numerous international awards, including the IEEE AP-S Young Professional Ambassador 2023, the IEEE AP-S Raj Mittra Travel Grant 2023, the EuCAP 2023 Best Antenna Paper Award, the IET Innovation Award in 2018, and the BAE Systems Chairman's Award in 2017. Additionally, he has served as a Session Chair and/or TPC Member for various conferences, including EuCAP2018, IEEE AP-S Symposium 2021, IEEE VTC2022-Fall, EuCAP2023, IEEE AP-S Symposium 2023, and EuCAP2024. He has consistently contributed as a reviewer for esteemed journals such as the *Nature Electronics*, *Nature Communications*, *Advanced Materials*, *Advanced Functional Materials*, and *Nano Energy*, in addition to reviewing for over 15 IEEE Transactions. He is a top-200 Reviewer for the IEEE TRANSACTIONS ON ANTENNA AND PROPAGATION from 2021 to 2023. He has also taken on the role of Guest Editor for prestigious publications, including the IEEE OPEN JOURNAL OF ANTENNAS AND PROPAGATION, *IET Electronic Letters*, *Micromachines*, and *Wireless Communications and Mobile Computing*, and an Associate Editor of the *Frontiers in Communications and Networks*.

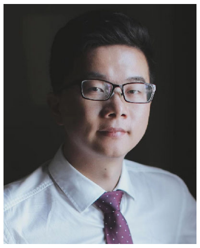

Lei Wang (Senior Member, IEEE) received the Ph.D. degree in electromagnetic field and microwave technology from Southeast University, Nanjing, China, in 2015.

From November 2017 to February 2020, he was an Alexander von Humboldt Scholar at the Institute of Electromagnetic Theory, Hamburg University of Technology (TUHH), Hamburg, Germany. Since March 2020, he has been an Assistant Professor at the Institute of Signals, Sensors and Systems, Heriot-Watt University, Edinburgh, U.K. His research interests include antenna theory and applications, active electronically scanning arrays, integrated antennas and arrays, substrate-integrated waveguide antennas, leaky-wave antennas, and wireless propagations.

Dr. Wang was awarded the Chinese National Scholarship for Ph.D. Candidates in 2014 and granted the Swiss Government Excellence Scholarship to conduct research at EPFL in 2014. He was also granted by the Alexander von Humboldt Research Foundation to take research at TUHH in 2016. Moreover, he received the Best Poster Award in the 2018 IEEE International Workshop on Antenna Technology (iWAT) and the Best Paper Award in the 5th International Conference on the Uc (UCET2020).

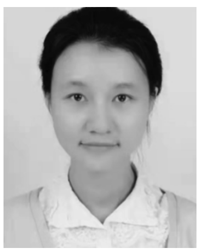

Ping Lu (Member, IEEE) received the B.S. degree in electrical engineering and automation from Southwest Jiaotong University, Chengdu, China, in 2012, and the Ph.D. degree in radio physics from the University of Electronic Science and Technology, Chengdu, in 2018.

From 2015 to 2017, she was a Joint Ph.D. Student Scholar with the Laboratoire Ampére, École Centrale de Lyon, INSA de Lyon, Université Claude Bernard de Lyon, Villeurbanne, France. She is currently an Associate Professor with the School of Electronics and Information Engineering, Sichuan University, Chengdu. Her current research interests include rectennas, nondiffraction beams, and wireless power transmission.

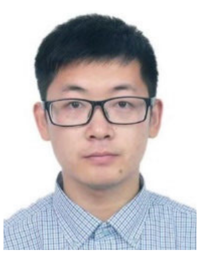

Cheng Zhang (Member, IEEE) was born in Henan, China. He received the M.S. degree in material science and technology from the Wuhan University of Technology, Wuhan, China, in 2015, and the Ph.D. degree from the State Key Laboratory of Millimeter Waves, Department of Radio Engineering, Southeast University, Nanjing, China, in 2019.

He is currently a Professor at the Shanghai Institute of Optics and Fine Mechanics, Chinese Academy of Sciences, Shanghai, China. He has authored or coauthored more than 50 publications (including six highly cited articles), with citation over 1500 times. His current research interests are EM energy harvesting, stealth metamaterial/metasurface, and multiphysical manipulation.

Dr. Zhang was a recipient of the 2020 China Top Cited Paper Award from IOP Publishing and Top Articles in Device Physics for *Applied Physics Letters* (two articles). He received the Honor Mention Award for the Best Student Paper Contest in the 2018 IEEE International Workshop on Antenna Technology (iWAT) and the Appreciation Award of Invited Talk in 2018 IEEE International Conference on Computational Electromagnetics (ICCEM).

Zhensheng Chen received the B.Eng. and M.Sc. degrees in communication engineering from Lanzhou University, Lanzhou, China, in 2015 and 2018, respectively. He is currently pursuing the Ph.D. degree with KU Leuven, Leuven, Belgium.

He joined Heriot-Watt University, Edinburgh, U.K., as a Visiting Ph.D. Researcher, in April 2022. His current research interests include wearable antennas, rectifying antennas, wireless power transfer (WPT), and RF energy harvesting (EH).

Xuezhi Zheng (Member, IEEE) received the M.S. degree in electrical engineering and the Ph.D. degree (summa cum laude) from KU Leuven, Leuven, Belgium, in 2010 and 2014, respectively.

From 2020 to 2021, he was a Visiting Scholar with the Cavendish Laboratory, Nanophotonics Centre, University of Cambridge, Cambridge, U.K. Since 2014, he has been a Post-Doctoral Researcher with the ESAT-WaveCore Group, KU Leuven. He is currently a Visiting Scholar with the Center for Polariton-Driven Light–Matter Interaction (POLIMA), Southern Denmark University, Odense, Denmark. His current research interests include the modeling of the interaction of electromagnetic (EM) waves with nanoscopic structures.

Yejun He (Senior Member, IEEE) received the Ph.D. degree in information and communication engineering from the Huazhong University of Science and Technology (HUST), Wuhan, China, in 2005.

From 2005 to 2006, he was a Research Associate with the Department of Electronic and Information Engineering, The Hong Kong Polytechnic University, Hong Kong. From 2006 to 2007, he was a Research Associate with the Department of Electronic Engineering, Faculty of Engineering, The Chinese University of Hong Kong, Hong Kong. In 2012, he was a Visiting Professor with the Department of Electrical and Computer Engineering, University of Waterloo, Waterloo, ON, Canada. From 2013 to 2015, he was an Advanced Visiting Scholar (Visiting Professor) with the School of Electrical and Computer Engineering, Georgia Institute of Technology, Atlanta, GA, USA. Since 2011, he has been a Full Professor with the College of Electronics and Information Engineering, Shenzhen University, Shenzhen, China, where he is the Director of the Guangdong Engineering Research Center of Base Station Antennas and Propagation and the Shenzhen Key Laboratory of Antennas and Propagation. He was selected as a Pengcheng Scholar Distinguished Professor, Shenzhen, and a Minjiang Scholar Chair Professor of Fujian, China, in 2020 and 2022, respectively. He has authored or coauthored over 260 research articles and seven books, and holds about 20 patents. His research interests include wireless communications, antennas, and radio frequency.

Dr. He is a fellow of IET and a Senior Member of the China Institute of Communications and the China Institute of Electronics. He was a recipient of the Shenzhen Overseas High-Caliber Personnel Level B ("Peacock Plan Award" B) and the Shenzhen High-Level Professional Talent (Local Leading Talent). He received the Shenzhen Science and Technology Progress Award in 2017 and the Guangdong Provincial Science and Technology Progress Award two times in 2018 and 2023. He is currently the Chair of the IEEE Antennas and Propagation Society-Shenzhen Chapter and obtained the 2022 IEEE APS Outstanding Chapter Award. He has served as a Reviewer for various journals, such as the IEEE TRANSACTIONS ON VEHICULAR TECHNOLOGY, IEEE TRANSACTIONS ON COMMUNICATIONS, IEEE TRANSACTIONS ON INDUSTRIAL ELECTRONICS, IEEE TRANSACTIONS ON ANTENNAS AND PROPAGATION, IEEE WIRELESS COMMUNICATIONS, IEEE COMMUNICATIONS LETTERS, *International Journal of Communication Systems*, *Wireless Communications and Mobile Computing*, and *Wireless Personal Communications*. He has also served as a Technical Program Committee Member or a Session Chair for various conferences, including the IEEE Global Telecommunications Conference (GLOBECOM), the IEEE International Conference on Communications (ICC), the IEEE Wireless Communication Networking Conference (WCNC), APCAP, EUCAP, UCMMT, and the IEEE Vehicular Technology Conference (VTC). He served as the TPC Chair for IEEE ComComAp 2021, the General Chair for IEEE ComComAp 2019, the TPC Co-Chair for WOCC 2023/2022/2019/2015, and an Organizing Committee Vice Chair for the International Conference on Communications and Mobile Computing (CMC 2010). He acted as the Publicity Chair for several international conferences, such as the IEEE PIMRC 2012. He is the Principal Investigator for over 30 current or finished research projects, including the National Natural Science Foundation of China, the Science and Technology Program of Guangdong Province, and the Science and Technology Program of Shenzhen City. He is serving as an Associate Editor for the IEEE TRANSACTIONS ON ANTENNAS AND PROPAGATION, IEEE TRANSACTIONS ON MOBILE COMPUTING, IEEE ANTENNAS AND PROPAGATION MAGAZINE, IEEE ANTENNAS AND WIRELESS PROPAGATION LETTERS, *International Journal of Communication Systems*, *China Communications*, and *Wireless Communications and Mobile Computing*. He served as an Associate Editor for the *Security and Communication Networks* journal and IEEE NETWORK.

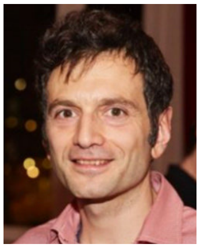

George Goussetis (Senior Member, IEEE) received the Diploma degree in electrical and computer engineering from the National Technical University of Athens, Athens, Greece, in 1998, the B.Sc. degree (Hons.) in physics from University College London, London, U.K., in 2002, and the Ph.D. degree from the University of Westminster, London, in 2002.

In 1998, he joined Space Engineering, Rome, Italy, as an RF Engineer. In 1999, he joined the Wireless Communications Research Group, University of Westminster, as a Research Assistant. From 2002 to 2006, he was a Senior Research Fellow with Loughborough University, Loughborough, U.K. He was a Lecturer (Assistant Professor) with Heriot-Watt University, Edinburgh, U.K., from 2006 to 2009, and a Reader (Associate Professor) with Queen's University Belfast, Belfast, U.K., from 2009 to 2013. In 2013, he joined Heriot-Watt University as a Reader and was promoted to a Professor in 2014, where he is currently the Director of the Institute of Sensors Signals and Systems. He has authored or coauthored over 500 peer-reviewed articles, five book chapters, one book, and four patents. His research interests are in the area of microwave and antenna components and subsystems.

Dr. Goussetis has held a research fellowship from the Onassis Foundation in 2001, a research fellowship from the U.K. Royal Academy of Engineering from 2006 to 2011, and European Marie-Curie experienced researcher fellowships in 2011 and 2012 and again in 2014 and 2017. He was a co-recipient of the 2011 European Space Agency Young Engineer of the Year Prize, the 2011 EuCAP Best Student Paper Prize, the 2012 EuCAP Best Antenna Theory Paper Prize, and the 2016 Bell Labs Prize. He has served as an Associate Editor for the IEEE ANTENNAS AND WIRELESS PROPAGATION LETTERS.

Guy A. E. Vandenbosch (Fellow, IEEE) received the M.S. and Ph.D. degrees in electrical engineering from Katholieke Universiteit Leuven, Leuven, Belgium, in 1985 and 1991, respectively.

From September to December 2014, he was a Visiting Professor with Tsinghua University, Beijing, China. Since 1993, he has been a Lecturer with Katholieke Universiteit Leuven, where he has been a Full Professor. His work has been published in ca. 400 articles in international journals and has led to ca. 425 papers at international conferences. His current research interests include the area of electromagnetic (EM) theory, computational electromagnetics, planar antennas and circuits, nano-EMs, EM radiation, electromagnetic compatibility (EMC), and bio-EMs.

Dr. Vandenbosch has been a member of the "Management Committees" of the consecutive European COST actions on antennas since 1993. Within the ACE Network of Excellence of the EU from 2004 to 2007, he was a member of the Executive Board and coordinated the activity on the creation of a European antenna software platform. From 2017 to 2020, he was a member of the IEEE Electromagnetics Award Committee. After ACE, from 2007 to 2018, he was the Chair of the EuRAAP Working Group on Software. He was a Vice-Chairman from 1999 to 2004, a Secretary from 2005 to 2009, and the Chairman from 2010 to 2017 of the IEEE Benelux Chapter on Antennas and Propagation. From 2002 to 2004, he was a Secretary of the IEEE Benelux Chapter on EMC. From 2012 to 2014, he was a Secretary of the Belgian National Committee for Radio-Electricity (URSI), where he is also in-charge of Commission.

Yi Huang (Fellow, IEEE) received the B.Sc. degree in physics from Wuhan University, Wuhan, China, in 1984, the M.Sc. (Eng.) degree in microwave engineering from the Nanjing Research Institute of Electronics Technology (NRIET), Nanjing, China, in 1987, and the D.Phil. degree in communications from the University of Oxford, Oxford, U.K., in 1994.

In 1994, he was a Research Fellow with British Telecom Laboratories, Ipswich, U.K. In 1995, he joined the Department of Electrical Engineering and Electronics, University of Liverpool, Liverpool, U.K., as a Faculty Member, where he is currently a Full Professor of wireless engineering, the Head of the High Frequency Engineering Group, and the Deputy Head of the Department. His experience includes three years with NRIET, as a Radar Engineer, and various periods with the University of Birmingham, Birmingham, U.K., the University of Oxford, and the University of Essex, Colchester, U.K., as a Research Staff Member. He has authored or coauthored more than 400 refereed articles in leading international journals and conference proceedings and authored three books, including a bestseller *Antennas: From Theory to Practice* (John Wiley, 2008 and 2021). He has received many patents and research grants from research councils, government agencies, charities, the EU, and industry. His research interests include antennas, wireless communications, applied electromagnetics, radar, and EMC, with a current focus on mobile antennas, wireless energy harvesting, and power transfer.

Dr. Huang was the U.K. and Ireland Representative of the European Association of Antenna and Propagation (EurAAP) from 2016 to 2020 and a fellow of IET. He was a recipient of more than ten awards, such as the BAE Systems Chairman's Award 2017, the IET, and the best paper awards. He was on a number of national and international technical committees and has been an Editor, an Associate Editor, or a Guest Editor of five international journals. He is the Editor-in-Chief of *Wireless Engineering and Technology* and has been an Associate Editor of the IEEE TRANSACTIONS ON ANTENNAS AND PROPAGATION since 2022 and an Associate Editor of the IEEE ANTENNAS AND WIRELESS PROPAGATION LETTERS from 2016 to 2022. In addition, he has been a Keynote or an Invited Speaker and an Organizer of many conferences and workshops, such as IEEE iWAT2010, LAPC2012, and EuCAP2018.